



# Generating independent chaotic attractors by chaos anticontrol in nonlinear circuits

Cristina Morel \*, Marc Bourcerie, François Chapeau-Blondeau

*Laboratoire d'Ingénierie des Systèmes Automatisés, Université d'Angers, 62 Avenue Notre Dame du Lac, 49000 Angers, France*

Accepted 4 January 2005

---

## Abstract

The present paper introduces a new technique to generate several independent chaotic attractors by designing a switching piecewise-constant controller in continuous-time systems. This controller can create chaos using an anticontrol of chaos feedback. It is shown that nonlinear continuous-time systems have several attractors, depending on initial conditions. We demonstrate that the state space equidistant repartition of these attractors is on a precise curve, that depends of the system parameters. A mathematical formula giving the distance between the attractors is then deduced. Finally, several examples are given to verify the proposed methodology.

© 2005 Elsevier Ltd. All rights reserved.

---

## 1. Introduction

Chaos has been extensively studied within the scientific, engineering and mathematical communities as an interesting complex dynamic phenomenon. Recently, the traditional trend of understanding and analyzing chaos has evolved to a new phase of investigation: controlling and utilizing chaos. Research in the field of chaos includes the suppression and the generation of chaos, e.g. generating chaotic attractors using a switching type of piecewise-linear controller [1–3]. For electronics engineers [4,5], it is well known that piecewise-linear functions can be used to generate various chaotic attractors such as  $n$ -scroll attractors in Chua's circuit [6]. A similar phenomenon generating various limit cycles is observed in [7,8]. In [7], two sets of the initial conditions produce two different limit cycles and a new limit cycle for each new initial condition selected is observed in [8]. Another technique to create chaos is the anticontrol of chaos (sometimes called chaotification), using time-delay feedback perturbation on a system parameter or employing an exogenous time-delay state-feedback input. The anticontrol reference method designs a simple nonlinear feedback controller with an arbitrarily small amplitude obtaining a chaotic dynamic in the controlled system [9–11].

The present paper proposes a new technique to generate several independent chaotic attractors, that can be reached from several different initial conditions. The initial system is chaotified using the new controller, which is a combination of the switching piecewise-constant characteristic and of the anticontrol of chaos state feedback (a simple sine function of the system state, as in [10]).

---

\* Corresponding author.

We demonstrate that the attractors periodicity in the state space depends on the sine anticontrol feedback frequency, thus enabling the determination of the distance between attractors. The study of the attractors repartition in the state space shows that they are situated on a precise curve. We determine the equation of this curve, which depends on the controlled system dynamics and on its parameters. To verify our methodology, we treat the well-known examples of Chua’s circuit, Lorenz system and the Buck converter.

A control engineering application is to make nonlinear system converge to some attractors of interest, starting from different initial conditions, in order to reach different regimes of operation.

**2. Generating independent chaotic attractors in a general nonlinear system**

Consider a  $N$ -dimensional nonlinear system in the general form of

$$\begin{cases} \dot{x}_1 = \sum_{i=1}^N a_i x_i + \sum_{i=1}^N b_{i,j} x_i x_j + \sum_{i=1}^N c_{i,j} x_i^2 x_j + v, \\ \dot{x}_2 = \sum_{i=1}^N m_i x_i + \sum_{i=1}^N n_{i,j} x_i x_j + \sum_{i=1}^N o_{i,j} x_i^2 x_j, \\ \vdots \\ \dot{x}_N = \sum_{i=1}^N q_i x_i + \sum_{i=1}^N r_{i,j} x_i x_j + \sum_{i=1}^N s_{i,j} x_i^2 x_j, \end{cases} \tag{1}$$

where  $a_i, b_{i,j}, c_{i,j}, m_i, n_{i,j}, o_{i,j}, q_i, r_{i,j}$  and  $s_{i,j}$ , for  $i, j = \overline{1, N}$ , are real parameters and  $v$  is zero.

A single-input controlled system is obtained by adding a feedback controller  $v$ . In order to generate independent chaotic attractors for the system (1), we specify a piecewise-constant characteristic for the feedback controller, defined analytically as follows:

$$v = \begin{cases} 1, & f(t) < u(t), \\ 0, & f(t) \geq u(t), \end{cases} \tag{2}$$

where  $f(t)$  is a periodic function with a small amplitude and  $u(t)$  the anticontrol of chaos state feedback. The application of the classical method ([9–11]) of anticontrol of chaos to obtain a chaotic dynamics in the controlled system (1) uses a simple nonlinear feedback with a small amplitude. We are interested in a simple sine function of the system state, as in [10], but with large variations of the sine amplitude. The nonlinear feedback is described by

$$u(t) = \varepsilon \sin(\sigma x_1(t)). \tag{3}$$

We propose to use the anticontrol of chaos state feedback together with a piecewise-constant controller, hereafter denoted anticontrol switching piecewise-constant controller.

Fig. 1 shows a transient state space trajectory until a chaotic attractor is reached. The transitions  $0 \rightarrow 1 \rightarrow 0 \rightarrow 1$  of the anticontrol switching piecewise-constant controller  $v$  of Eq. (2) determine a triangle characteristic of the transient state space trajectory. The times  $(t_k)_{k \in \mathbb{N}}$  of the transitions  $1 \rightarrow 0$  of  $v$  are symbolized by circles ● on the state space. At each time  $(t_k)_{k \in \mathbb{N}}$ ,  $f(t)$  is equal to  $u(t)$ . Consequently, we can write:

$$f(t) = u(t). \tag{4}$$

According with Eq. (3), Eq. (4) becomes:

$$f(t) = \varepsilon \sin(\sigma x_1(t)). \tag{5}$$

For  $t = t_0$ , the solution of Eq. (5) is:

$$x_1(t_0) = \frac{1}{\sigma} \arcsin \frac{f(t_0)}{\varepsilon}. \tag{6}$$

The  $2\pi$  periodicity of the sine function of  $u(t)$  enables to find all the solutions  $x_1(t_k)$  of Eq. (4):

$$\sigma x_1(t_k) \pm 2k\pi = \arcsin \frac{f(t_0)}{\varepsilon}, \quad k \in \mathbb{N}. \tag{7}$$

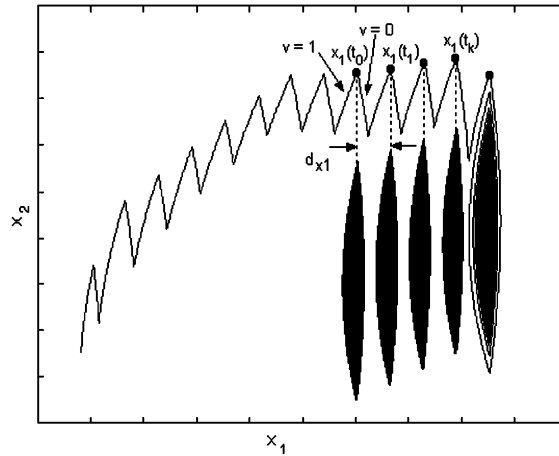


Fig. 1. Periodicity of the attractors in the state space.

Then,

$$x_1(t_k) = \frac{1}{\sigma} \arcsin \frac{f(t_0)}{\varepsilon} \pm \frac{2k\pi}{\sigma}, \quad k \in \mathbb{N}. \tag{8}$$

We can also write:

$$x_1(t_k) - x_1(t_{k-1}) = \frac{2\pi}{\sigma}, \quad k \in \mathbb{N}^+. \tag{9}$$

We have demonstrated that the periodicity of the  $x_1(t)$  function is  $2\pi/\sigma$ , i.e. the distance on the  $x_1$  axis between two consecutive transitions  $1 \rightarrow 0$  of  $v$ .

Fig. 1 presents several independent chaotic attractors reached from different initial conditions. These attractors have an equidistant repartition on the state space. Furthermore, we observe that the distance between two consecutive attractors on the  $x_1$  axis coincides with the distance between two circles ● on the  $x_1$  axis. Therefore, the distance between two consecutive attractors is:

$$d_{x_1} = \frac{2\pi}{\sigma}. \tag{10}$$

Choosing  $(x_{i0})_{i=1,N} = (x_i(0))_{i=1,N}$  as independent dynamical variables, the attractors are situated on a precise curve in the state space.

The equilibrium points of the system (1) are defined by:

$$\dot{x}_i = 0, \quad \text{for } i = \overline{1,N}. \tag{11}$$

Applying the Eq. (11) to the system (1) gives:

$$\left\{ \begin{array}{l} \sum_{i=1}^N a_i x_i + \sum_{i=1}^N \sum_{j=1}^N b_{i,j} x_i x_j + \sum_{i=1}^N c_{i,j} x_i^2 x_j + v = 0, \\ \sum_{i=1}^N m_i x_i + \sum_{i=1}^N \sum_{j=1}^N n_{i,j} x_i x_j + \sum_{i=1}^N \sum_{j=1}^N o_{i,j} x_i^2 x_j = 0, \\ \vdots \\ \sum_{i=1}^N q_i x_i + \sum_{i=1}^N \sum_{j=1}^N r_{i,j} x_i x_j + \sum_{i=1}^N \sum_{j=1}^N s_{i,j} x_i^2 x_j = 0. \end{array} \right. \tag{12}$$

When  $v$  varies, the equilibrium points of the system (12) are situated on a curve we name attractors curve. Indeed, the dynamical state space trajectory remains around the fixed point, for each attractor. Taking the last  $N - 1$  equations of the system (12) into account, the same curve is obtained, but the first parametrical equation of the system (12) is

eliminated. The attractors curve is given by the last  $N - 1$  implicit equations (12). Furthermore, Eq. (12) enables to determine the distance between two consecutive attractors on the other axis  $(x_i)_{i=2, \dots, N}$ . If one of the state variables  $(x_w)_{w=2, \dots, N}$  is explicit and presents a linear relation with the state variables  $(x_i)_{i=1, \dots, N}$ , substituting the state variable  $(x_i)_{i=1, \dots, N}$  by  $(d_{x_i})_{i=1, \dots, N}$  leads to the determination of  $(d_{x_w})_{w=2, \dots, N}$ , the distance between two consecutive attractors on the  $w$  axis.

In order to verify our independent chaotic attractors generation methodology, let us treat the well-known examples of Chua’s circuit, Lorentz system and the Buck converter.

**3. Chua’s circuit**

The Chua’s circuit [6,10] has become, in recent years, a standard model for the study of chaos in systems described by finite-dimensional differential equations. The state equations of Chua’s circuit are:

$$\begin{cases} \dot{x}_1 = \alpha(x_2 - x_1 - g(x_1)), \\ \dot{x}_2 = x_1 - x_2 + x_3, \\ \dot{x}_3 = -\beta x_2 - \gamma x_3, \end{cases} \tag{13}$$

where

$$g(x_1) = bx_1 + \frac{a-b}{2}(|x_1 + 1| - |x_1 - 1|). \tag{14}$$

With the dimensionless state (13), (14), when  $\alpha = 10$ ,  $\beta = 24.5$ ,  $\gamma = 0$ ,  $a = -1.27$  and  $b = -0.68$ , a stable period orbit of Chua’s circuit is generated, as in Fig. 2.

As discussed previously, in order to generate several independent chaotic attractors, we can apply the anticontrol switching piecewise-constant controller  $v$  of Eq. (2). The Chua’s circuit (13) becomes:

$$\begin{cases} \dot{x}_1 = \alpha(x_2 - x_1 - g(x_1, v)), \\ \dot{x}_2 = x_1 - x_2 + x_3, \\ \dot{x}_3 = -\beta x_2, \end{cases} \tag{15}$$

where

$$g(x_1, v) = bx_1 + v \frac{a-b}{2}(|x_1 + 1| - |x_1 - 1|). \tag{16}$$

The anticontrol switching piecewise-constant controller is chosen according with Eqs. (2) and (3), for  $\varepsilon = 50$ ,  $\sigma = 100$  and  $f(t) = \sin(1000t)$  as follows:

$$v = \begin{cases} 1, & \sin(1000t) < 50 \cdot \sin(100x_1) \\ 0, & \sin(1000t) \geq 50 \cdot \sin(100x_1). \end{cases} \tag{17}$$

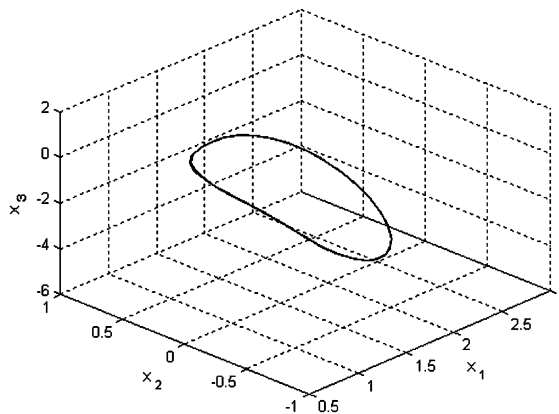


Fig. 2. A stable period orbit of Chua’s circuit (Eqs. (13) and (14)) with  $a = -1.27$ ,  $b = -0.68$ ,  $\alpha = 10$ ,  $\beta = 24.5$  and  $\gamma = 0$ .

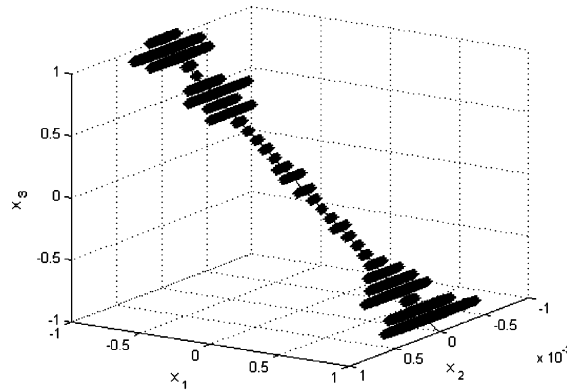


Fig. 3. Independent chaotic attractors of Chua's circuit of Eq. (15).

Fig. 3 displays several independent chaotic attractors in the state space. The same phenomena is observed even with other numerical values of  $\varepsilon$ ,  $\sigma$  and with any periodical function  $f(t)$ . The attractors are situated on a line, whose equation results from the application of (12) to the modified Chua's circuit (15):

$$\begin{cases} x_2 = 0, \\ x_3 = -x_1. \end{cases} \tag{18}$$

The equidistant repartition of the attractors on the state space enables to determine the distance between two consecutive attractors on the three axes. According to the Eq. (10) for the axis  $x_1$ , we have:

$$d_{x_1} = \frac{2\pi}{\sigma} = 0.0628. \tag{19}$$

To determine the distance between two consecutive independent chaotic attractors on the other axes  $x_2$  and  $x_3$ , the state variables of Eq. (18) are replaced by  $d_{x_2}$  and  $d_{x_3}$ :

$$\begin{cases} d_{x_2} = 0, \\ d_{x_3} = -d_{x_1} = -0.0628. \end{cases} \tag{20}$$

#### 4. Lorentz system

The Lorentz system [10] is described by

$$\begin{cases} \dot{x}_1 = -10x_1 + 10x_2, \\ \dot{x}_2 = rx_1 - x_2 - x_1x_3 + v, \\ \dot{x}_3 = -\frac{8}{3}x_3 + x_1x_2, \end{cases} \tag{21}$$

where  $v$  is zero. The uncontrolled Lorentz system (21) has the origin as an exponentially stable equilibrium point if  $0 < r \leq 1$ , two stable equilibria  $(\sqrt{8(r-1)}/3, \sqrt{8(r-1)}/3, r-1)$  and  $(-\sqrt{8(r-1)}/3, -\sqrt{8(r-1)}/3, r-1)$  if  $1 < r < r_H \approx 24.74$ . The Lorentz system is chaotic if  $r > r_H$ . In our simulations, we take  $r = 1$ . Using the anticontrol switching piecewise-constant controller (17), the Lorentz system (21) presents several independent chaotic attractors as shown in Fig. 4. The attractors are situated on the following curve:

$$\begin{cases} x_2 = x_1, \\ x_3 = \frac{3x_1x_2}{8}. \end{cases} \tag{22}$$

The distance between two consecutive attractors on the axes  $x_1$  and  $x_2$  is given by Eq. (22) and (10).

$$\begin{cases} d_{x_1} = \frac{2\pi}{\sigma} = 0.0628, \\ d_{x_2} = d_{x_1} = 0.0628. \end{cases} \tag{23}$$

Even if the state variable  $x_3$  is explicit,  $d_{x_3}$  cannot be determined, because Eq. (22) is not linear.

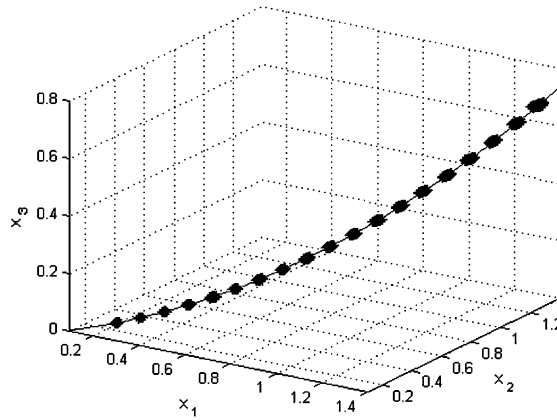


Fig. 4. Independent chaotic attractors of the Lorentz system (21).

**5. The Buck converter**

Fig. 5 shows the diagram of a classical Buck converter that uses a piecewise-constant characteristic as feedback controller [4,12]. The circuit has two states determined by the position of the switch  $S$ . When  $S$  is closed, the input voltage  $E$  provides energy to the load  $R$  as well as to the inductor  $L$ . When  $S$  is open, the inductor current  $x_2$ , which flows through diode  $D$ , transfers some of its stored energy to the load  $R$ . The amplifier  $A_2$  has a gain  $A$ . The simplest feedback converter is obtained when the control law  $v_{c2}(t)$  is identically zero. The control law  $v_c(t)$  can then be written in function of the voltage  $x_1$  of the capacitor  $C$ :

$$v_c(t) = v_{c1}(t) = A(x_1(t) - V_{ref}). \tag{24}$$

The control law  $v_c(t)$  is applied to the inverting input of the comparator  $A_1$ . The non-inverting input is connected to an independent voltage ramp generator. This ramp voltage  $v_r(t)$  can be expressed as

$$v_r(t) = V_L + (V_U - V_L) \frac{t \bmod T}{T}. \tag{25}$$

When  $v_c(t) \geq v_r(t)$ , the switch  $S$  is open and diode  $D$  conducts; otherwise  $S$  is closed and  $D$  is blocked. The voltage  $x_1$  of the capacitor  $C$  and the inductance current  $x_2$  are chosen as state variables [13,14]. The model of the converter can be written as

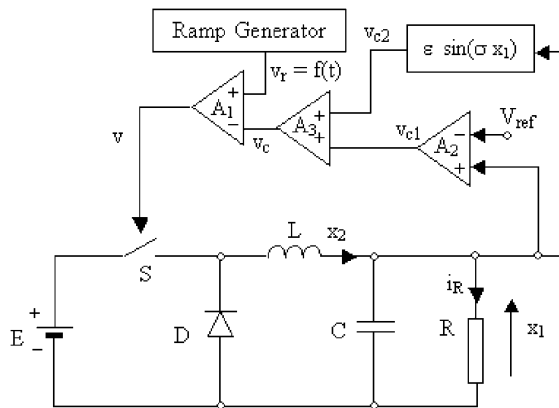


Fig. 5. Block diagram of the Buck converter with a feedback anticontrol.

$$\dot{x}_1 = -\frac{1}{RC}x_1 + \frac{1}{C}x_2, \tag{26}$$

$$\dot{x}_2 = -\frac{1}{L}x_1 + \frac{E}{L}v, \tag{27}$$

where

$$v = \begin{cases} 0, & v_r(t) < A(x_1(t) - E), \\ 1, & v_r(t) \geq A(x_1(t) - E). \end{cases} \tag{28}$$

and  $E$  is a constant input voltage. This classical converter has been studied for many years, notably in [4,12–14]. We decided to choose the same values as in these references:  $L = 20$  mH,  $C = 47$   $\mu$ F,  $R = 22$   $\Omega$ ,  $A = 8.4$ ,  $V_{ref} = 11.3$  V,  $V_L = 3.8$  V,  $V_U = 8.2$  V,  $T = 400$   $\mu$ s and  $E = 16$  V.

Because the Buck converter uses a piecewise-constant characteristic described by Eq. (28) as feedback controller, we only have to apply Eq. (3) to generate independent chaotic attractors. The new control law we propose has the expression:

$$v_c(t) = v_{c1}(t) + v_{c2}(t) = A(x_1(t) - V_{ref}) + \varepsilon \sin[\sigma(x_1(t) - V_{ref})]. \tag{29}$$

The anticontrol switching piecewise-constant controller is:

$$v = \begin{cases} 0, & f(t) < A(x_1(t) - V_{ref}) + \varepsilon \cdot \sin(\sigma(x_1(t) - V_{ref})), \\ 1, & f(t) \geq A(x_1(t) - V_{ref}) + \varepsilon \cdot \sin(\sigma(x_1(t) - V_{ref})), \end{cases} \tag{30}$$

where  $f(t) = v_r(t)$ ,  $\varepsilon = 18$  V and  $\sigma = 100$  rad/V.

The attractors are situated on a line, whose equation results from the application of Eq. (12) in Eq. (26):

$$x_2 = \frac{1}{R}x_1. \tag{31}$$

The slope of the line attractors only depends on the converter load resistance  $R$ . The variation of the load resistance  $R$  (12  $\Omega$ , 16  $\Omega$ , 22  $\Omega$ , 30  $\Omega$ ), displays on the Fig. 6 several independent chaotic attractors, reached from different initial conditions.

Using (10) and (31), the distance between two consecutive attractors is determined.

$$d_{x_1} = \frac{2\pi}{\sigma} = 0.0628 \text{ V}. \tag{32}$$

$$d_{x_2} = \frac{2\pi}{R\sigma} = 0.014 \text{ A}. \tag{33}$$

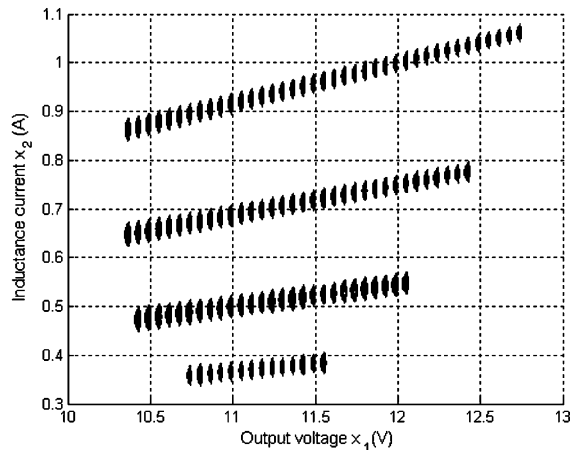


Fig. 6. Attractors diagram using different initial conditions in function of  $R$ :  $R = 12 \Omega, 16 \Omega, 22 \Omega, 30 \Omega$ .

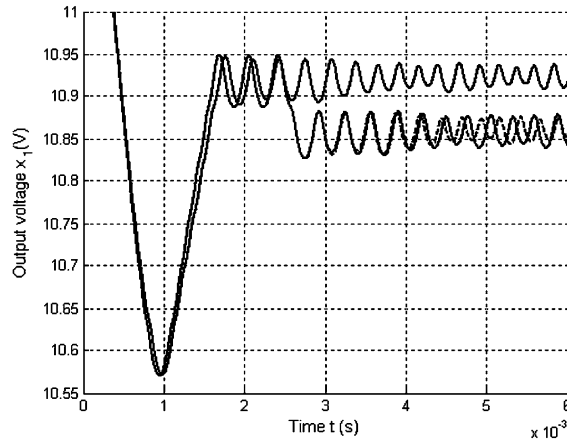


Fig. 7. Sensitive dependence on initial conditions of the Buck converter (26), (27) and (30) starting from  $(x_{10}; x_{20}) = (11.4004; 0.48)$ ,  $(x_{10}; x_{20}) = (11.4005; 0.48)$  and  $(x_{10}; x_{20}) = (11.4006; 0.48)$ .

The sensitive dependence on initial conditions of the modified Buck converter (26), (27) and (30) is a generic property of chaotic systems. Fig. 7 presents three time trajectories starting from distinct, but almost identical, initial conditions  $(x_{10}; x_{20}) = (11.4004; 0.48)$ ,  $(x_{10}; x_{20}) = (11.4005; 0.48)$  and  $(x_{10}; x_{20}) = (11.4006; 0.48)$ . At the beginning (i.e. for  $t = 0$ ), the trajectories are undistinguishable. After a few iterations, the sequences differ widely, even if the initial conditions differ less than 0.001%. Starting from  $(x_{10}; x_{20}) = (11.4004; 0.48)$  and  $(x_{10}; x_{20}) = (11.4005; 0.48)$ , the trajectories are close one from the other, remain in the same bounded region around  $x_1 = 10.86$  V, but never coincide. With  $(x_{10}; x_{20}) = (11.4006; 0.48)$ , the time trajectory ends in the other bounded region (around  $x_1 = 10.925$  V).

A quantitative measure of the sensitive dependence on initial conditions is the Lyapunov exponent. Considering  $\varepsilon$  as parameter, the maximum Lyapunov exponent of the modified Buck converter (26), (27) and (30) is shown in Fig. 8. Its positive value shows the chaotical behavior of the Buck converter.

We study the attractors repartition in the state space as a function of the parameter  $\varepsilon$ . Without any changes of the Buck converter parameters ( $R, L, C, \dots$ ), all the chaotic attractors are situated on the same curve on the state space when  $\varepsilon$  varies, because  $R$  is fixed. In order to avoid the superposition of the attractors in a graphical  $(x_1; x_2)$  state space representation, we decide to represent them according to the state variable  $x_2$  and the parameter  $\varepsilon$  in Fig. 9. For  $\varepsilon < 12$ , the Buck converter is characterized by a unique attractor. The system presents several independent chaotic attractors, reached from many different initial conditions, for  $\varepsilon \geq 12$  V.

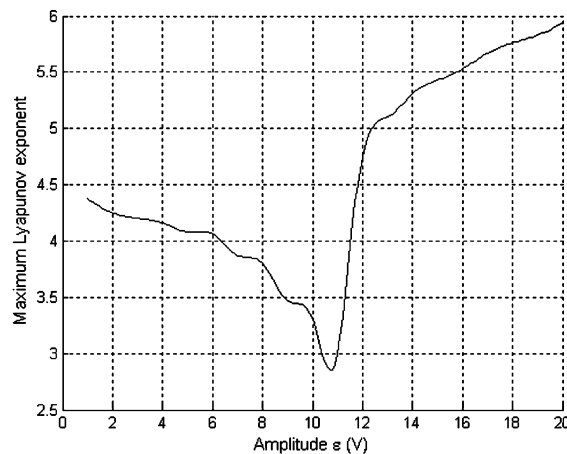


Fig. 8. The maximum Lyapunov exponent of Buck converter (26), (27) and (30) in function of  $\varepsilon$ .

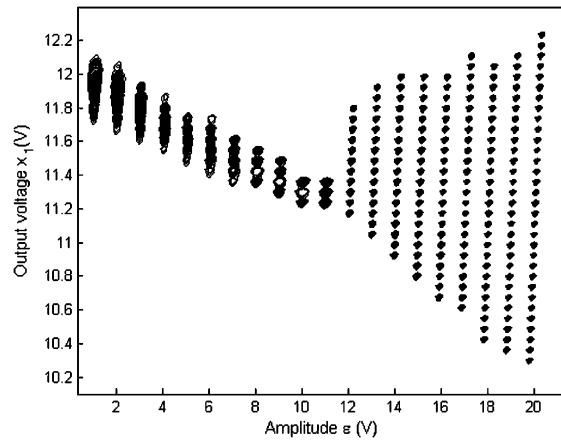


Fig. 9. Attractors diagram in function of  $\varepsilon$ , with different initial conditions.

## 6. Conclusion

The present paper introduces a new technique to generate several independent chaotic attractors by designing a new controller, which is a combination of the switching piecewise-constant characteristic and of the anticontrol of chaos state feedback.

We demonstrated that the attractors periodicity in the state space depends on the sine anticontrol feedback frequency, thus enabling the determination of the distance between attractors, which repartition in the state space is on a precise curve. We determined the equation of this curve, which depends on the controlled system dynamics and on its parameters.

A control engineering application is to make nonlinear system converge to some attractors of interest, starting from different initial conditions, in order to reach different regimes of operation.

## References

- [1] Lu J, Yu X, Chen G. Generating chaotic attractors with multiple merged basins of attraction: a switching piecewise-linear control approach. *IEEE Trans Circ Syst I* 2003;50:198–207.
- [2] Lu J, Yu X, Zhou T, Chen G, Yang X. Generating chaos with a switching piecewise-linear controller. *Chaos* 2002;12:344–9.
- [3] Aziz-Alaoui M, Chen G. Asymptotic analysis of a new piecewise-linear chaotic system. *Int J Bifurcation Chaos* 2002;12:147–57.
- [4] Tse C. *Complex behavior of switching power converters*. New York: CRC Press; 2003.
- [5] Chen G, Ueta T. *Chaos in circuits and systems*. London: World Scientific; 2002.
- [6] Tang W, Zhong G, Chen G, Man K. Generation of N-scoll attractors via sine function. *IEEE Trans Circ Syst I* 2001;48:1369–72.
- [7] Kennedy M. Three steps to chaos—part I: evolution. *IEEE Trans Circ Syst I* 1993;40:640–56.
- [8] Endersen L, Skarland N. Limit cycle oscillations in pacemaker cells. *IEEE Trans Biomed Eng* 2000;47:1–5.
- [9] Li Z, Park J, Chen G, Young H, Choi Y. Generating chaos via feedback control from a stable ts fuzzy system through a sinusoidal nonlinearity. *Int J Bifurcation Chaos* 2002;12:2283–91.
- [10] Wang X, Chen G, Yu X. Anticontrol of chaos in continuous-time systems via time-delay feedback. *Chaos* 2000;10:771–9.
- [11] Morel C, Bourcerie M, Chapeau-Blondeau F. Improvement of power supply electromagnetic compatibility by expansion of chaos anticontrol. *J Circ, Syst & Comput* 2005;14, in press.
- [12] Fossas E, Olivar G. Study of chaos in the Buck converter. *IEEE Trans Circ Syst I* 1996;43:13–25.
- [13] di Bernardo M, Garofalo F, Glielmo L, Vasca F. Switchings, bifurcations, and chaos in DC–DC converters. *IEEE Trans Circ Syst I* 1998;45:133–41.
- [14] Hamill D, Deane J, Jefferies D. Modeling of chaotic DC–DC converters by iterated nonlinear mappings. *IEEE Trans Power Electron* 1992;7:25–36.